

## Effects of spontaneous emission on nondispersing wave packets in two-electron atoms

Birgit S. Mecking<sup>1</sup> and P. Lambropoulos<sup>1,2</sup>

<sup>1</sup>Max-Planck-Institut für Quantenoptik, Hans-Kopfermann-Strasse 1, D-85748 Garching, Germany

<sup>2</sup>Foundation for Research and Technology Hellas, Institute of Electronic Structure and Laser,

P.O. Box 1527, Heraklion 71110, Crete, Greece

(Received 8 August 1997)

We investigate the Rydberg wave packet dynamics of core-driven two-electron atoms with the density matrix formalism. The spontaneous emission of the core transition is included. We show how it modifies the dynamics of radial Rydberg wave packets, which are nondispersing, but slowly decaying in the absence of spontaneous emission. Although our considerations apply to all two-electron atoms, we focus on the experimentally convenient element calcium. [S1050-2947(98)07003-6]

PACS number(s): 32.80.Rm, 32.80.Dz, 42.50.Ct

### I. INTRODUCTION

In the last two years, the suppression of dispersion of radial Rydberg wave packets in two-electron atoms has been proposed and investigated theoretically [1,2]. The basic concept is the application of two laser pulses: a short one exciting the radial Rydberg wave packet and a second one driving the core after the excitation. This technique is sometimes called isolated core excitation (ICE) and its effect on wave packet dynamics has been the subject of many recent publications [3–6]. The core resonant field causes Rabi oscillations between the Rydberg series, to which the wave packet is excited originally, and an upper lying autoionizing Rydberg series. Nevertheless, autoionization hardly occurs, if the Rabi oscillation and the Kepler-like motion of the radial Rydberg wave packet are synchronized in a proper way, that is, if the core is in its ground state whenever the Rydberg wave packet is at its inner turning radius. At that moment, autoionization is impossible, since the atomic energy is below the first ionization threshold. On the other hand, whenever the Rydberg electron is sufficiently far away from the core, the configuration interaction between electron and core is weak and the atom hardly autoionizes, even if the core is in its excited state. Conditions for the required synchronization are a good timing between exciting and core resonant laser pulse, and the choice of the Rabi period as a small integer multiple of the Kepler period. The stabilization of the Rydberg wave packet against dispersion can now be understood in terms of the necessity to fulfill the timing condition; i.e., when the wave packet broadens, the tails are no longer synchronized and therefore undergo autoionization, whereas the center is still well timed and therefore almost unaffected by autoionization. Thus it is understandable that the setup under consideration leads to slowly decaying, nondispersing Rydberg wave packets.

It is now important to ask how this effect is influenced by the spontaneous emission of the core transition. Semiclassically speaking, the spontaneous emission of one photon at an arbitrary moment destroys the above mentioned timing, by changing the phase of the Rabi oscillation. Consequently, spontaneous emission of the core transition is expected to have a negative effect on the stabilization of the Rydberg wave packet [2]. Nevertheless, in a first approach the system

was examined by using amplitude equations and thereby neglecting the spontaneous emission [1]. This approximation is valid as long as the radiative lifetime of the core

$$\tau(\text{a.u.}) = 1/\Gamma(\text{a.u.}) \quad (1)$$

is long compared to the Kepler period

$$T_{cl}(\text{a.u.}) \approx 2\pi\langle\nu\rangle^3 \quad (2)$$

[7], where  $\Gamma$  is the decay rate of the core transition and  $\langle\nu\rangle$  the mean quantum number of the wave packet. In order to get a feeling for the orders of magnitude involved, let us turn to the example of calcium with its decay rate  $\Gamma = 3.79 \times 10^{-9}$  a.u. (see Appendix). The corresponding radiative lifetime  $\tau = 6.38$  ns is much longer than the Kepler period  $T_{cl} \approx 20$  ps of a wave packet centered around  $\langle\nu\rangle = 50$ , and the problem can be treated without caring about spontaneous emission. This effect is important only for much higher mean quantum numbers where the Kepler period is comparable to (or even exceeds) the radiative lifetime of the core transition. But the latter case is the more interesting one, as soon as the classical features of Rydberg atoms are considered.

Thus a thorough investigation of the phenomenon including spontaneous deexcitation of the core is desirable. It requires the extension of our previous formalism so as to include this mechanism, as well as a realistic calculation for the quantitative assessment of the importance of the effect in a specific context. The issue has also been raised and investigated by Zobay and Alber [2], whose formulation in terms of multichannel quantum defect theory (MQDT) required a Monte Carlo type of approach since their equations were cast in terms of the channel wave functions. We have chosen to generalize our previous approach, which was cast in terms of the resolvent operator for the wave function, by deriving the corresponding set of density matrix equations into which spontaneous decay can be incorporated relatively straightforwardly. As we shall see later on, the number of the necessary differential equations is quite reasonable, presenting no particular difficulty in their numerical solution. In addition to its relevance to the problem at hand, this set of density matrix equations represents a master equation in which two incoherent mechanisms (reservoirs) such as spontaneous decay and transitions to the atomic continuum coexist. This approach is

possible here only because autoionization can be formulated in terms of discrete states and the respective continua to which they are coupled. And it is the isolated core excitation arrangement of the problem, which creates a series of separate resonances, that allows such a treatment. The additional cross coupling of these resonances by the laser is also readily included in the equations.

At this point, it is relevant to recall earlier work, almost 20 years ago, in which the question of interference between radiative emission and autoionization in the decay of atomic states excited above the first ionization threshold was formulated and discussed by Armstrong *et al.* [8]. At the time, the authors recognized that such phenomena would be of relevance only in stripped ions of relatively high  $Z$  where autoionizing and radiative lifetimes become comparable. For neutral atoms, however, typical autoionizing lifetimes, at least of states normally within experimental resolution, are much shorter than radiative decay, unless of course one considers autoionizing states involving at least one electron at an orbit of very high principal quantum number, say  $\nu \cong 200$ , which is practically unattainable spectroscopically. What makes our problem relevant to neutral atoms is the involvement of a wave packet and not of a single autoionizing state. Spectroscopically, this requires the excitation of a band of high Rydberg states which is readily accomplished experimentally. If it became possible to resolve single autoionizing states of sufficiently high  $\nu$  (see also discussion in Sec. III), then the considerations of Ref. [8] would be of experimental relevance even for neutral atoms.

Another difference between that work and the present paper lies in the intention. Here we are concerned with the interplay between a wave packet and two reservoirs and not with the features of the spectra of the emitted photons and electrons which was the chief concern of Ref. [8]. Our formalism is nevertheless capable of dealing with those questions as well and is in fact more general in that it includes a manifold of states and the respective continua. Having in addition the master equation, one can deal with the implications of the Rabi oscillation in driving the autoionizing states strongly and its effect on the spectra, if one chose to do so.

In that respect, our work is also related to papers that appeared in the early 1980s (see, for example, [9,10], and references therein), whose concern was the inclusion of radiative decay in strongly driven autoionizing states. Master equations were also formulated in those papers which addressed the effect of strong driving on the photoemission spectra. Again the difference in our work is that we deal with manifolds (instead of one) of autoionizing states and the wave packet aspects.

Thus in some sense our work unifies and generalizes the above discussed earlier papers, in addition to providing a realistic and quantitative context to assess the possible relevance of those earlier formal considerations to present-day experimental possibilities. It may be useful to remind the reader here that even the effect of the strong driving on autoionizing line shapes was observed for the first time only recently [11], 15 years after the initial prediction [12–14]. It is interesting to ponder when the interplay between photoelectron and photoemission spectra might be observed. Our discussion of the relevant lifetimes in Sec. III does provide a quantitative frame of assessment. These are in fact issues we

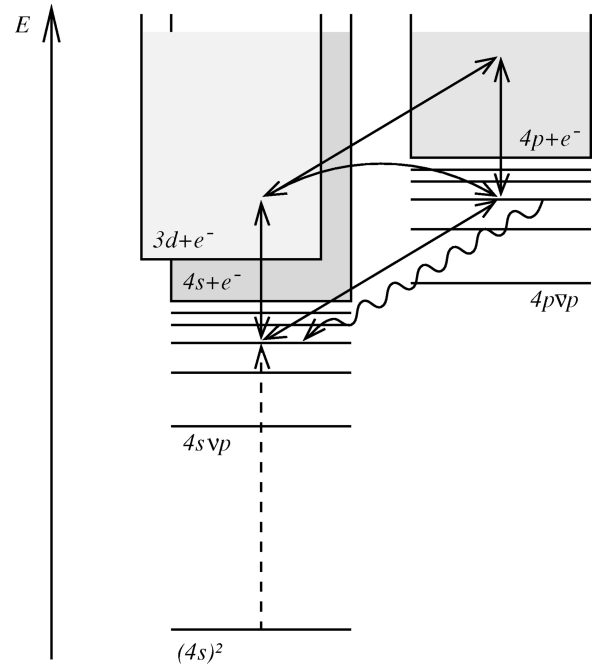


FIG. 1. Level scheme of calcium with the relevant interactions: dashed arrow:  $D_{\text{ex}}$ ; straight arrows:  $D$ ; curved arrow:  $V$ .

intend to discuss in a separate publication not dealing with wave packets, which is our main concern here.

Since calcium is a promising candidate for experimental investigation of the effect [15], we will focus our attention on this alkaline earth element. Referring to calcium, Fig. 1 shows the ground state  $|g\rangle = |(4s)^2\rangle$ , the nonautoionizing Rydberg states  $|\nu\rangle = |4s\nu p\rangle$  and the autoionizing Rydberg states  $|\bar{\nu}\rangle = |4p\bar{\nu}p\rangle$ , as well as the relevant continuum states  $|c_1\rangle = |4s+e^-(\epsilon_{c_1})\rangle$ ,  $|c_2\rangle = |3d+e^-(\epsilon_{c_2})\rangle$ , and  $|\bar{c}\rangle = |4p+e^-(\epsilon_{\bar{c}})\rangle$  with the corresponding free electron energies  $\epsilon_{c_{1,2}}$  and  $\epsilon_{\bar{c}}$ . A special feature of calcium is the autoionization of the upper Rydberg series into two independent continua, namely, the  $4s$ -continuum  $|c_1\rangle$  and the  $3d$ -continuum  $|c_2\rangle$ . Our formalism, which is introduced in Sec. II, takes the configuration coupling of  $|\bar{\nu}\rangle$  to two independent continua into account and is therefore appropriate for calcium. For our numerical calculations, shown in Sec. III, we used values that are reasonably accurate in the case of calcium.

## II. FORMULATION

In this section we outline the derivation of the density matrix equations describing the dynamics of the ground state and the Rydberg states.

The Hamiltonian of the system consists of the atomic part  $H^{\text{atom}}$ , whose eigenstates are  $\{|n\rangle\} = \{|g\rangle, \{|\nu\rangle\}, \{|\bar{\nu}\rangle\}, \{|c_{1,2}\rangle\}, \{|\bar{c}\rangle\}\}$ , the configuration coupling  $V$ , and the time-dependent interactions  $D^{\text{ex}}(t)$  and  $D(t)$  of the atom with the laser pulses (see Fig. 1). We start our calculations by considering the Liouville equation

$$i\hbar \dot{\rho} = [H, \rho] = [H^{\text{atom}} + V + D^{\text{ex}} + D, \rho] \quad (3)$$

for the atom coupled to the external fields and expanding it in the full basis of states  $\{|n\rangle\}$ . This procedure gives a system of first order differential equations for the corresponding density matrix elements. The introduction of the spontaneous emission of the core transition with rate  $\Gamma$  yields

$$i\hbar\dot{\rho}_{gg} = \dots, \quad (4a)$$

$$i\hbar\dot{\rho}_{vg} = (E_v - E_g)\rho_{vg} + \dots, \quad (4b)$$

$$i\hbar\dot{\rho}_{\bar{v}g} = (E_{\bar{v}} - E_g - i\Gamma/2)\rho_{\bar{v}g} + \dots, \quad (4c)$$

$$i\hbar\dot{\rho}_{c_{1,2}g} = (E_{c_{1,2}} - E_g)\rho_{c_{1,2}g} + \dots, \quad (4d)$$

$$i\hbar\dot{\rho}_{c_g} = (E_c - E_g - i\Gamma/2)\rho_{c_g} + \dots, \quad (4e)$$

$$i\hbar\dot{\rho}_{v_1v_2} = (E_{v_1} - E_{v_2})\rho_{v_1v_2} + i\Gamma\delta_{v_1,v_2}\rho_{\bar{v}_1\bar{v}_2} + \dots, \quad (4f)$$

$$i\hbar\dot{\rho}_{\bar{v}_1v_2} = (E_{\bar{v}_1} - E_{v_2} - i\Gamma/2)\rho_{\bar{v}_1v_2} + \dots, \quad (4g)$$

$$i\hbar\dot{\rho}_{c_{1,2}v} = (E_{c_{1,2}} - E_v)\rho_{c_{1,2}v} + \dots, \quad (4h)$$

$$i\hbar\dot{\rho}_{c_v} = (E_c - E_v - i\Gamma/2)\rho_{c_v} + \dots, \quad (4i)$$

$$i\hbar\dot{\rho}_{\bar{v}_1\bar{v}_2} = (E_{\bar{v}_1} - E_{\bar{v}_2} - i\Gamma)\rho_{\bar{v}_1\bar{v}_2} + \dots, \quad (4j)$$

$$i\hbar\dot{\rho}_{c_{1,2}\bar{v}} = (E_{c_{1,2}} - E_{\bar{v}} - i\Gamma/2)\rho_{c_{1,2}\bar{v}} + \dots, \quad (4k)$$

$$i\hbar\dot{\rho}_{c_v\bar{v}} = (E_c - E_{\bar{v}} - i\Gamma)\rho_{c_v\bar{v}} + \dots, \quad (4l)$$

where  $E_n = \langle n|H^{\text{atom}}|n\rangle$  denote the atomic energies and  $\delta_{v_1,v_2}$  is the Kronecker symbol. In order to save space, the parts of the equations which contain the coupling to all the other populations and coherences and where the matrix elements  $V_{n_1n_2}$ ,  $D_{n_1n_2}^{\text{ex}}$ , and  $D_{n_1n_2}$  appear are not written down here. In principle, one could derive the way  $\Gamma$  enters the equations by considering the vacuum field as well. But this is a well-known procedure [16] and needs not be repeated here. The above equations imply that it is convenient to change to slowly varying density matrix elements

$$\sigma_{n_1n_2} = \rho_{n_1n_2} e^{i\omega_{n_1n_2}t}, \quad (5)$$

with  $\omega_{n_1n_2}$  being one of the frequencies out of  $\{0, \omega_{\text{ex}}, \omega, \omega_{\text{ex}} + \omega, \omega_{\text{ex}} + 2\omega\}$  which is nearest the energy difference  $E_{n_1} - E_{n_2}$ . Let  $\mu_{n_1n_2}$  be the dipole matrix element between the states  $|n_1\rangle$  and  $|n_2\rangle$  and  $\mathcal{E}^{\text{ex}}(t)$  and  $\mathcal{E}(t)$  be the envelopes of the exciting and core resonant laser pulses. Thus the system of equations can be simplified by writing the matrix elements

$$D_{n_1n_2}^{\text{ex}}(t) = \mu_{n_1n_2} [\mathcal{E}^{\text{ex}}(t) e^{-i\omega_{\text{ex}}t} + \text{c.c.}], \quad (6a)$$

$$D_{n_1n_2}(t) = \mu_{n_1n_2} [\mathcal{E}(t) e^{-i\omega t} + \text{c.c.}] \quad (6b)$$

in dipole approximation and by applying the rotating wave approximation. In the resulting system of equations the continuum is eliminated adiabatically [17,18]. Thus we obtain the integrals

$$\sum_{j=1,2} \lim_{\epsilon \rightarrow 0} \int dc_j \frac{|\mu_{c_jv}\mathcal{E}|^2}{E_v + \hbar\omega - E_{c_j} + i\epsilon} =: S_v - \frac{i}{2} \gamma_v, \quad (7a)$$

$$\sum_{j=1,2} \lim_{\epsilon \rightarrow 0} \int dc_j \frac{|V_{c_jv}|^2}{E_v + \hbar\omega - E_{c_j} + i\epsilon} + \int d\bar{c} \frac{|\mu_{c\bar{v}}\mathcal{E}|^2}{E_v + 2\hbar\omega - E_{\bar{c}} + i\Gamma/2} =: S_{\bar{v}} - \frac{i}{2} \gamma_{\bar{v}}, \quad (7b)$$

$$\sum_{j=1,2} \lim_{\epsilon \rightarrow 0} \int dc_j \frac{\mu_{v_1c_j}\mu_{c_jv_2}|\mathcal{E}|^2}{E_{v_3} + \hbar\omega - E_{c_j} + i\epsilon} =: \Omega_{v_1v_2} \left(1 - \frac{i}{q_{v_1v_2}}\right), \quad (7c)$$

$v_1 \neq v_2$

$$\sum_{j=1,2} \lim_{\epsilon \rightarrow 0} \int dc_j \frac{V_{\bar{v}_1c_j}V_{c_j\bar{v}_2}}{E_{v_3} + \hbar\omega - E_{c_j} + i\epsilon} + \int d\bar{c} \frac{\mu_{\bar{v}_1\bar{c}}\mu_{\bar{c}\bar{v}_2}|\mathcal{E}|^2}{E_{v_3} + 2\hbar\omega - E_{\bar{c}} + i\Gamma/2} =: \Omega_{\bar{v}_1\bar{v}_2} \left(1 - \frac{i}{q_{\bar{v}_1\bar{v}_2}}\right), \quad \bar{v}_1 \neq \bar{v}_2 \quad (7d)$$

$$\mu_{\bar{v}_1v_2}\mathcal{E} + \sum_{j=1,2} \lim_{\epsilon \rightarrow 0} \int dc_j \frac{V_{\bar{v}_1c_j}\mu_{c_jv_2}\mathcal{E}}{E_{v_3} + \hbar\omega - E_{c_j} + i\epsilon} =: \Omega_{\bar{v}_1v_2} \left(1 - \frac{i}{q_{\bar{v}_1v_2}}\right), \quad (7e)$$

where we used the well-known formula

$$\lim_{\epsilon \rightarrow 0} \frac{1}{E_v + \hbar\omega - E_c + i\epsilon} = \mathcal{P} \frac{1}{E_v + \hbar\omega - E_c} - i\pi\delta(E_v + \hbar\omega - E_c) \quad (8)$$

to split up the corresponding integrals into their real and imaginary parts [13] and where  $E_{v_3}$  is an average energy within the manifold of the Rydberg states. Discussion in more detail of such integrals coupling discrete states to each other via continua can be found in Ref. [17]. There are also similar integrals with slightly different denominators: either  $E_v$  is replaced by  $E_g + \hbar\omega_{\text{ex}}$ , or  $E_v + \hbar\omega$  is replaced by  $E_{\bar{v}} + i\Gamma/2$ . In the first case we make no further distinction, since we assume that  $E_g + \hbar\omega_{\text{ex}} \approx E_v$  for all significantly populated states  $|v\rangle$ . In the second case the quantities belonging to the integrals with a larger imaginary part of the denominator are marked by a tilde. Defining  $\Omega_{n_1n_2}^{\text{ex}} := \mu_{n_1n_2}\mathcal{E}^{\text{ex}}$ , we obtain

$$\dot{\sigma}_{gg} = \frac{i}{\hbar} \left[ \sum_{\nu'} \Omega_{\nu'g}^{\text{ex}} \sigma_{g\nu'} - \sum_{\nu'} \Omega_{g\nu'}^{\text{ex}} \sigma_{\nu'g} \right], \quad (9a)$$

$$\begin{aligned} \dot{\sigma}_{\nu g} = & \frac{i}{\hbar} \left[ \left( (E_g + \hbar \omega_{\text{ex}}) - (E_\nu + S_\nu) + \frac{i}{2} \gamma_\nu \right) \sigma_{\nu g} - \Omega_{\nu g}^{\text{ex}} \sigma_{gg} \right. \\ & - \sum_{\nu' \neq \nu} \Omega_{\nu\nu'} \left( 1 - \frac{i}{q_{\nu\nu'}} \right) \sigma_{\nu'g} - \sum_{\nu'} \Omega_{\nu\nu'} \\ & \left. \times \left( 1 - \frac{i}{q_{\nu\nu'}} \right) \sigma_{\nu'g} + \sum_{\nu'} \Omega_{\nu'g}^{\text{ex}} \sigma_{\nu\nu'} \right], \quad (9b) \end{aligned}$$

$$\begin{aligned} \dot{\sigma}_{\bar{\nu}g} = & \frac{i}{\hbar} \left[ \left( (E_g + \hbar \omega_{\text{ex}} + \hbar \omega) - (E_{\bar{\nu}} + S_{\bar{\nu}}) + \frac{i}{2} (\gamma_{\bar{\nu}} + \Gamma) \right) \sigma_{\bar{\nu}g} \right. \\ & - \sum_{\nu'} \Omega_{\bar{\nu}\nu'} \left( 1 - \frac{i}{q_{\bar{\nu}\nu'}} \right) \sigma_{\nu'g} - \sum_{\bar{\nu}' \neq \bar{\nu}} \Omega_{\bar{\nu}\bar{\nu}'} \\ & \left. \times \left( 1 - \frac{i}{q_{\bar{\nu}\bar{\nu}'}} \right) \sigma_{\bar{\nu}'g} + \sum_{\nu'} \Omega_{\nu'g}^{\text{ex}} \sigma_{\bar{\nu}\nu'} \right], \quad (9c) \end{aligned}$$

$$\begin{aligned} \dot{\sigma}_{\nu_1\nu_2} = & \frac{i}{\hbar} \left[ \left( (E_{\nu_2} + S_{\nu_2}) - (E_{\nu_1} + S_{\nu_1}) + \frac{i}{2} (\gamma_{\nu_1} + \gamma_{\nu_2}) \right) \sigma_{\nu_1\nu_2} \right. \\ & - i\Gamma \delta_{\nu_1,\nu_2} \sigma_{\bar{\nu}_1\bar{\nu}_2} - \Omega_{\nu_1g}^{\text{ex}} \sigma_{g\nu_2} - \sum_{\nu' \neq \nu_1} \Omega_{\nu_1\nu'} \\ & \times \left( 1 - \frac{i}{q_{\nu_1\nu'}} \right) \sigma_{\nu'\nu_2} - \sum_{\bar{\nu}'} \Omega_{\nu_1\bar{\nu}'} \left( 1 - \frac{i}{q_{\nu_1\bar{\nu}'}} \right) \sigma_{\bar{\nu}'\nu_2} \\ & + \Omega_{g\nu_2}^{\text{ex}} \sigma_{\nu_1g} + \sum_{\nu' \neq \nu_2} \Omega_{\nu'\nu_2} \left( 1 + \frac{i}{q_{\nu'\nu_2}} \right) \sigma_{\nu_1\nu'} \\ & \left. + \sum_{\bar{\nu}'} \Omega_{\bar{\nu}'\nu_2} \left( 1 + \frac{i}{q_{\bar{\nu}'\nu_2}} \right) \sigma_{\nu_1\bar{\nu}'} \right], \quad (9d) \end{aligned}$$

$$\begin{aligned} \dot{\sigma}_{\bar{\nu}_1\bar{\nu}_2} = & \frac{i}{\hbar} \left[ \left( (E_{\nu_2} + \tilde{S}_{\nu_2} + \hbar \omega) - (E_{\bar{\nu}_1} + S_{\bar{\nu}_1}) + \frac{i}{2} (\gamma_{\bar{\nu}_1} + \tilde{\gamma}_{\nu_2} \right. \right. \\ & \left. \left. + \Gamma) \right) \sigma_{\bar{\nu}_1\bar{\nu}_2} - \sum_{\nu'} \Omega_{\bar{\nu}_1\nu'} \left( 1 - \frac{i}{q_{\bar{\nu}_1\nu'}} \right) \sigma_{\nu'\nu_2} \right. \\ & - \sum_{\bar{\nu}' \neq \bar{\nu}_1} \Omega_{\bar{\nu}_1\bar{\nu}'} \left( 1 - \frac{i}{q_{\bar{\nu}_1\bar{\nu}'}} \right) \sigma_{\bar{\nu}'\nu_2} + \Omega_{g\nu_2}^{\text{ex}} \sigma_{\bar{\nu}_1g} \\ & + \sum_{\nu' \neq \nu_2} \tilde{\Omega}_{\nu'\nu_2} \left( 1 + \frac{i}{\tilde{q}_{\nu'\nu_2}} \right) \sigma_{\bar{\nu}_1\nu'} + \sum_{\bar{\nu}'} \tilde{\Omega}_{\bar{\nu}'\nu_2} \\ & \left. \times \left( 1 + \frac{i}{\tilde{q}_{\bar{\nu}'\nu_2}} \right) \sigma_{\bar{\nu}_1\bar{\nu}'} \right], \quad (9e) \end{aligned}$$

$$\begin{aligned} \dot{\sigma}_{\bar{\nu}_1\bar{\nu}_2} = & \frac{i}{\hbar} \left[ \left( (E_{\bar{\nu}_2} + \tilde{S}_{\bar{\nu}_2}) - (E_{\bar{\nu}_1} + \tilde{S}_{\bar{\nu}_1}) + \frac{i}{2} (\tilde{\gamma}_{\bar{\nu}_1} + \tilde{\gamma}_{\bar{\nu}_2}) \right. \right. \\ & \left. \left. + i\Gamma \right) \sigma_{\bar{\nu}_1\bar{\nu}_2} - \sum_{\nu'} \tilde{\Omega}_{\bar{\nu}_1\nu'} \left( 1 - \frac{i}{\tilde{q}_{\bar{\nu}_1\nu'}} \right) \sigma_{\nu'\bar{\nu}_2} \right. \\ & - \sum_{\bar{\nu}' \neq \bar{\nu}_1} \tilde{\Omega}_{\bar{\nu}_1\bar{\nu}'} \left( 1 - \frac{i}{\tilde{q}_{\bar{\nu}_1\bar{\nu}'}} \right) \sigma_{\bar{\nu}'\bar{\nu}_2} + \sum_{\nu'} \tilde{\Omega}_{\nu'\bar{\nu}_2} \\ & \times \left( 1 + \frac{i}{\tilde{q}_{\nu'\bar{\nu}_2}} \right) \sigma_{\bar{\nu}_1\nu'} + \sum_{\bar{\nu}' \neq \bar{\nu}_2} \tilde{\Omega}_{\bar{\nu}'\bar{\nu}_2} \\ & \left. \times \left( 1 + \frac{i}{\tilde{q}_{\bar{\nu}'\bar{\nu}_2}} \right) \sigma_{\bar{\nu}_1\bar{\nu}'} \right]. \quad (9f) \end{aligned}$$

This system of equations for the slowly varying density matrix elements is now ready to be investigated numerically.

### III. RESULTS

In the following, some of our results concerning calcium are presented.

In order to examine the atomic dynamics, we integrate the above equations numerically with the initial condition of the whole population being originally in the ground state. We choose the number  $\Delta\nu$  of included quantum numbers around  $\langle\nu\rangle$  such that the inclusion of any further level leaves the results unchanged. In our particular calculations, whose results are shown below,  $\Delta\nu=55$  levels are taken into account and therefore a system of  $(2\Delta\nu+1)^2=12321$  real equations has to be solved. Concerning the laser pulses, we use a Gaussian-shaped envelope  $\mathcal{E}^{\text{ex}}(t)$  centered around  $t=0$  with a width  $\Delta t=T_{\text{cl}}/3$  for the exciting pulse and a Heaviside step function  $\mathcal{E}(t)=\mathcal{E}_0\Theta(t-T_{\text{cl}})$  for the envelope of the core resonant pulse. That is, we assume that the core-driving laser field is, for the purpose of this investigation, switched on one Kepler period after the maximum of the exciting pulse has been reached and then stays constant. The exciting pulse is tuned to the energy difference between the states  $|g\rangle$  and  $|\langle\nu\rangle\rangle$ , i.e.,  $\omega_{\text{ex}}=(E_{\langle\nu\rangle}+S_{\langle\nu\rangle}-E_g)/\hbar$  and the core resonant pulse to the energy difference between  $|\langle\nu\rangle\rangle$  and  $|\langle\bar{\nu}\rangle\rangle$ , i.e.,  $\omega=(E_{\langle\bar{\nu}\rangle}+S_{\langle\bar{\nu}\rangle}-E_{\langle\nu\rangle}-\tilde{S}_{\langle\nu\rangle})/\hbar$ . The intensity of the core resonant laser is chosen such that the stabilization effect is maximal, i.e., that the Rabi period matches the Kepler period. All other parameters, which are used in order to obtain the graphs shown, are listed in the Appendix. Of course, in experiments, pulsed lasers of appropriately longer duration will be used for the core transition as well, as has been discussed in [1].

Figures 2 and 3 refer to a wave packet which is originally excited around  $\langle\nu\rangle=50$ . We obtain optimal stabilization for  $\mathcal{E}_0=2.04\times 10^{-6}$  a.u., which corresponds to an intensity of  $I=0.58$  MW/cm<sup>2</sup>. In Fig. 2 the spontaneous emission of the core transition is neglected, that is,  $\Gamma=0$ . Since this is the same assumption as in [1], graph 2 is similar to the results shown in that paper, although we have included here the configuration coupling of the upper Rydberg series to a second continuum. The total population of the wave packet, i.e.,

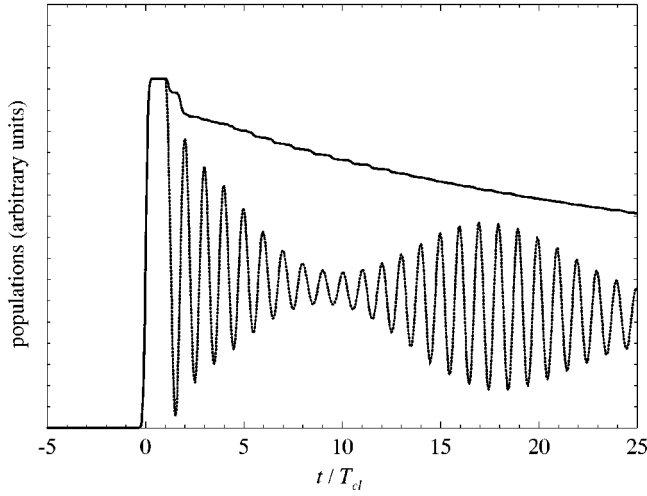


FIG. 2. Population of the wave packet (full curve) and total population of the lower Rydberg series (dotted curve) in the case of  $\langle \nu \rangle = 50$  and  $\Gamma = 0$ .

the sum of the populations of all Rydberg states, shows the following behavior: After the core resonant laser pulse is switched on at  $t = T_{cl}$  the total excited population decreases fast in the beginning, which means that parts of the wave packet are autoionized until the shape of the wave packet is consistent with the above explained scheme of synchronization between wave packet and core dynamics. After a few Kepler periods, the stabilization effect reaches its full extent and we observe only very little autoionization. The coherence between wave packet and core dynamics is reflected in the total population of the lower Rydberg series which shows a structure similar to one collapse and one half revival within a period of  $1/2 T_{rev}$ , where  $T_{rev} \approx 2\langle \nu \rangle T_{cl}/3$  is the wave packet's revival time [7], approximately  $33 T_{cl}$  in our case. Figure 3 refers to the realistic decay rate  $\Gamma = 3.79 \times 10^{-9}$  a.u. of calcium (see Appendix), where the radiative lifetime  $\tau = 6.38$  ns is much longer than the Kepler period  $T_{cl} \approx 20$  ps.

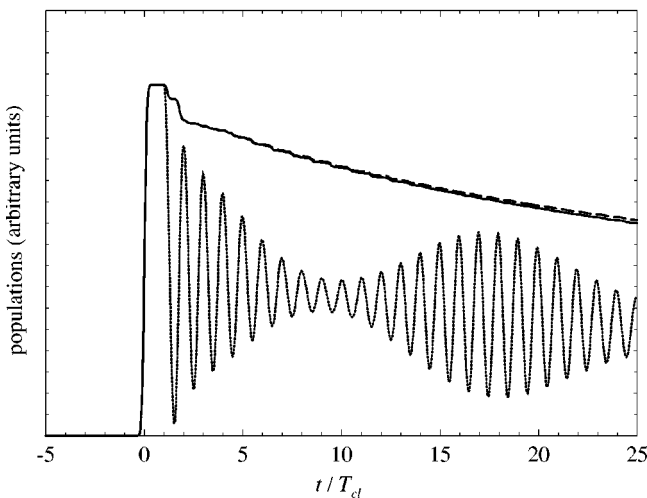


FIG. 3. Population of the wave packet (full curve) and total population of the lower Rydberg series (dotted curve) in the case of  $\langle \nu \rangle = 50$  and  $\Gamma = 3.79 \times 10^{-9}$  a.u. For comparison, the population of the wave packet in the case  $\langle \nu \rangle = 50$  and  $\Gamma = 0$  is also plotted (dashed curve).

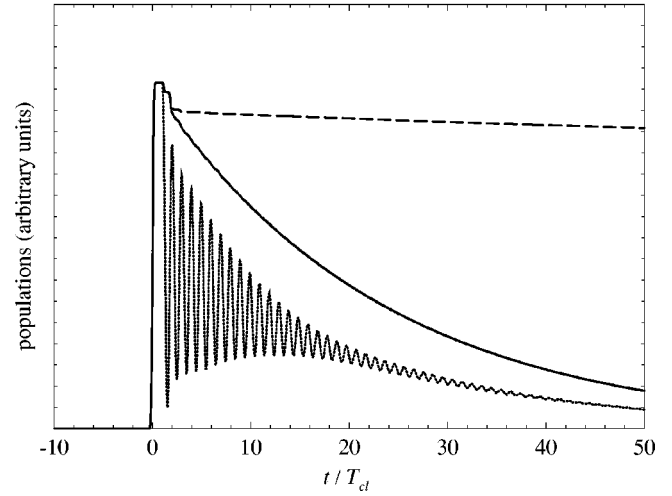


FIG. 4. Population of the wave packet (full curve) and total population of the lower Rydberg series (dotted curve) in the case of  $\langle \nu \rangle = 200$  and  $\Gamma = 3.79 \times 10^{-9}$  a.u. For comparison, the population of the wave packet in the case  $\langle \nu \rangle = 200$  and  $\Gamma = 0$  is also plotted (dashed curve).

As one can expect from the small ratio  $T_{cl}/\tau \approx 3.1 \times 10^{-3}$ , the effect of spontaneous emission is small: the decay of the total population of the Rydberg series is slightly faster than in Fig. 2, but the wave packet is still stabilized during many Kepler orbits.

In contrast, Fig. 4 shows a wave packet with  $\langle \nu \rangle = 200$ , whose Kepler period  $T_{cl} \approx 1.2$  ns has the same order of magnitude as  $\tau$  and leads to a considerable size of the ratio  $T_{cl}/\tau \approx 0.19$ . In this case optimal stabilization is obtained for  $\mathcal{E}_0 = 2.93 \times 10^{-8}$  a.u. ( $I = 0.12$  kW/cm<sup>2</sup>). The most striking difference in comparison to Figs. 2 and 3 is that the population of the wave packet decays much faster as soon as spontaneous emission of the core transition is taken into account, that is, autoionization is no longer suppressed effectively. This result is in good accordance with [2], where the parameters chosen for the numerical example they examined correspond to the case  $T_{cl}/\tau = 0.2$ . Additionally, we wish to focus attention on the fact that in Fig. 4 the structure of collapses and revivals in the total population of the lower Rydberg series disappears after several Kepler orbits and gives way to an incoherent, statistical superposition of the ground and the excited state of the core. This reflects the fact that the spontaneous emission of the core transition introduces a stochastic component, thereby destroying the coherence between wave packet and core dynamics. There is no longer a fixed phase relation between the Kepler-like motion of the wave packet and the Rabi oscillation of the core, and stabilization due to judicious synchronization is no longer possible.

#### IV. CONCLUSION

We have recast the results of [1], concerning nondispersing radial Rydberg wave packets in core-driven two-electron atoms, by using the density operator formalism. Starting from this, the spontaneous emission of the core transition has been included. We showed that it destroys in general the coherence between the wave packet and the core dynamics

and therefore has a negative effect on the stabilization of the wave packet against autoionization and dispersion. But we saw also that the magnitude of the influence of the spontaneous emission depends strongly on the ratio between Kepler period  $T_{cl}$  and radiative lifetime of the core transition  $\tau$ . In our concrete example of calcium, the inclusion of spontaneous emission has proved to be important only for very high mean quantum numbers of roughly  $\langle \nu \rangle > 100$ , where the Kepler period  $T_{cl}$  is sufficiently large. It would nevertheless be interesting to contemplate experiments even in that regime, as they would address a rather novel situation in which a wave packet interacts with two reservoirs.

### ACKNOWLEDGMENTS

One of us (B.S.M.) wishes to acknowledge the financial support by the Deutsche Forschungsgemeinschaft. We thank O. Zobay and G. Alber for interesting discussions and for making their manuscripts available to us prior to publication, as well as M. Strehle, U. Weichmann, and G. Gerber for continuing discussions on the experimental aspects of the problem.

### APPENDIX: ATOMIC PARAMETERS

Most of the atomic parameters appearing in our equations were determined by performing atomic structure calculations for small and moderate quantum numbers and by extrapolating the obtained values to higher quantum numbers via QDT formulas. As we do not want to occupy too much space by listing all the numbers used in our numerical calculations, we confine ourselves only to the extrapolating QDT formulas

$$E_\nu + \tilde{S}_\nu \approx E_\nu + S_\nu \approx -0.436\,278\,5 - 0.5(\nu - 1.84)^{-2}, \quad (\text{A1})$$

$$E_{\bar{\nu}} + \tilde{S}_{\bar{\nu}} \approx E_{\bar{\nu}} + S_{\bar{\nu}} \approx -0.320\,820\,0 - 0.5(\bar{\nu} - 2.00)^{-2}, \quad (\text{A2})$$

$$\mu_{\nu g} = \mu_{g\nu} \approx 1.7434(\nu - 1.84)^{-3/2}, \quad (\text{A3})$$

$$\gamma_\nu^{4s} \approx 7\mathcal{E}_0^2(\nu - 1.84)^{-3}, \quad (\text{A4})$$

$$\gamma_\nu^{3d} \approx 4\mathcal{E}_0^2(\nu - 1.84)^{-3}, \quad (\text{A5})$$

$$\gamma_\nu^{4s} \approx 0.1350(\bar{\nu} - 2.00)^{-3}, \quad (\text{A6})$$

$$\gamma_\nu^{3d} \approx 0.1247(\bar{\nu} - 2.00)^{-3}, \quad (\text{A7})$$

and the formulas used to determine the remaining atomic parameters

$$\tilde{\gamma}_\nu \approx \gamma_\nu = \gamma_\nu^{4s} + \gamma_\nu^{3d}, \quad (\text{A8})$$

$$\tilde{\gamma}_{\bar{\nu}} \approx \gamma_{\bar{\nu}} = \gamma_{\bar{\nu}}^{4s} + \gamma_{\bar{\nu}}^{3d}, \quad (\text{A9})$$

$$\Gamma = \frac{4}{3 \times 137^3} \omega^3 \mu_0^2, \quad [3], \quad (\text{A10})$$

$$\tilde{\Omega}_{\nu\nu'} \approx \Omega_{\nu\nu'} = 0 = \Omega_{\bar{\nu}\bar{\nu}'} \approx \tilde{\Omega}_{\bar{\nu}\bar{\nu}'}, \quad (\text{A11})$$

$$\begin{aligned} \tilde{\Omega}_{\bar{\nu}\nu'} = \tilde{\Omega}_{\nu'\bar{\nu}} \approx \Omega_{\bar{\nu}\nu'} = \Omega_{\nu'\bar{\nu}} = \mathcal{E}_0 \mu_0 \\ \times (-1)^{\nu' - \bar{\nu}} \frac{\sin \pi(\nu' - \bar{\nu} + 0.16)}{\pi(\nu' - \bar{\nu} + 0.16)}, \quad [19], \end{aligned} \quad (\text{A12})$$

$$\frac{\tilde{\Omega}_{\nu_1\nu_2}}{\tilde{q}_{\nu_1\nu_2}} \approx \frac{\Omega_{\nu_1\nu_2}}{q_{\nu_1\nu_2}} = \frac{1}{2} (\sqrt{\gamma_{\nu_1}^{4s} \gamma_{\nu_2}^{4s}} + \sqrt{\gamma_{\nu_1}^{3d} \gamma_{\nu_2}^{3d}}), \quad (\text{A13})$$

$$\frac{\tilde{\Omega}_{\bar{\nu}_1\bar{\nu}_2}}{\tilde{q}_{\bar{\nu}_1\bar{\nu}_2}} \approx \frac{\Omega_{\bar{\nu}_1\bar{\nu}_2}}{q_{\bar{\nu}_1\bar{\nu}_2}} = \frac{1}{2} (\sqrt{\gamma_{\bar{\nu}_1}^{4s} \gamma_{\bar{\nu}_2}^{4s}} + \sqrt{\gamma_{\bar{\nu}_1}^{3d} \gamma_{\bar{\nu}_2}^{3d}}), \quad (\text{A14})$$

$$\begin{aligned} \frac{\tilde{\Omega}_{\bar{\nu}\nu'}}{\tilde{q}_{\bar{\nu}\nu'}} = \frac{\tilde{\Omega}_{\nu'\bar{\nu}}}{\tilde{q}_{\nu'\bar{\nu}}} \approx \frac{\Omega_{\bar{\nu}\nu'}}{q_{\bar{\nu}\nu'}} = \frac{\Omega_{\nu'\bar{\nu}}}{q_{\nu'\bar{\nu}}} = \frac{1}{2} (-1)^{\nu' - \bar{\nu}} (\sqrt{\gamma_{\nu'}^{4s} \gamma_{\bar{\nu}}^{4s}} \\ + \sqrt{\gamma_{\nu'}^{3d} \gamma_{\bar{\nu}}^{3d}}), \end{aligned} \quad (\text{A15})$$

where  $\mu_0 = 2.18$ . All of the above numbers are given in atomic units. Although we do not claim high accuracy, these values are reasonably good for calcium, especially for the design of experiments, and are also compatible with experimental data where available [20–22].

[1] Lars G. Hanson and P. Lambropoulos, Phys. Rev. Lett. **74**, 5009 (1995).  
 [2] O. Zobay and G. Alber, Phys. Rev. A **54**, 5361 (1996); for a related problem in a somewhat different context, see also K. Hornberger and A. Buchleitner, Europhys. Lett. (to be published).  
 [3] Thomas F. Gallagher, *Rydberg Atoms* (Cambridge University Press, Cambridge, England, 1994).  
 [4] O. Zobay and G. Alber, Phys. Rev. A **52**, 541 (1995).  
 [5] F. Robicheaux, Phys. Rev. A **47**, 1391 (1993).  
 [6] Xiao Wang and W. E. Cooke, Phys. Rev. Lett. **67**, 976 (1991).  
 [7] I. Sh. Averbukh and N. F. Perelman, Phys. Lett. A **139**, 449 (1989).

[8] Lloyd Armstrong, Jr., Constantine E. Theodosiou, and M. J. Wall, Phys. Rev. A **18**, 2538 (1978).  
 [9] Joseph W. Haus, Maciej Lewenstein, and Kazimierz Rzażewski, Phys. Rev. A **28**, 2269 (1983).  
 [10] G. S. Agarwal, S. L. Haan, and J. Cooper, Phys. Rev. A **29**, 2552 (1984); **29**, 2565 (1984).  
 [11] N. E. Karapanagioti, O. Faucher, Y. L. Shao, D. Charalambidis, H. Bachau, and E. Cormier, Phys. Rev. Lett. **74**, 2431 (1995); N. E. Karapanagioti, D. Charalambidis, C. J. G. C. Uiterwaal, C. Fotakis, H. Bachau, I. Sanchez, and E. Cormier, Phys. Rev. A **53**, 2587 (1996).  
 [12] P. Lambropoulos, Appl. Opt. **19**, 3926 (1980).  
 [13] P. Lambropoulos and P. Zoller, Phys. Rev. A **24**, 379 (1981).

- [14] K. Rzazewski and J. H. Eberly, *Phys. Rev. Lett.* **47**, 408 (1981); *Phys. Rev. A* **27**, 2026 (1983).
- [15] M. Strehle, U. Weichmann, and G. Gerber (private communication).
- [16] C. Cohen-Tannoudji, J. Dupont-Roc, and G. Grynberg, *Atom-Photon Interactions* (John Wiley & Sons, New York, 1992).
- [17] S. N. Dixit and P. Lambropoulos, *Phys. Rev. A* **27**, 861 (1983).
- [18] Takashi Nakajima and P. Lambropoulos, *Phys. Rev. A* **50**, 595 (1994).
- [19] S. A. Bhatti, C. L. Cromer, and W. E. Cooke, *Phys. Rev. A* **24**, 161 (1981).
- [20] J. Sugar and C. Corliss, *J. Phys. Chem. Ref. Data* **14**, 51 (1985).
- [21] W. L. Wiese, M. W. Smith, and B. M. Miles, *Atomic Transition Probabilities* (U.S. Government Printing Office, Washington, D.C., 1969).
- [22] A. Bolovinos, E. Luc-Koenig, S. Assimopoulos, A. Lyras, N. E. Karapanagioti, D. Charalambidis, and M. Aymar, *Z. Phys. D* **38**, 265 (1996).